PHYSICAL REVIEW E VOLUME 60, NUMBER 6 DECEMBER 1999

Rescaling invariance and anomalous transport in a stochastic layer

S. S. Abdullaev* and K. H. Spatschek
Institut für Theoretische Physik I, Heinrich-Heine-Universität Düsseldorf, D-40225 Düsseldorf, Germany
(Received 4 May 1999)

The anomalous chaotic transport in a one-degree-of-freedom Hamiltonian system subjected to a small time-periodic perturbation is investigated. Strong quasiperiodic dependencies of the statistical properties of the motion on $\log \epsilon$ are found, where ϵ is a perturbation parameter. The period $\log \lambda$ depends on the rescaling parameter λ, which is determined only by the frequency of perturbation and behavior of unperturbed Hamiltonian near a saddle point. The results confirm and generalize a recently established new universal rescaling property of perturbed motion near a saddle point. [S1063-651X(99)51712-1]

PACS number(s): 05.45.Ac, 05.60.Cd

Anomalous transport is one of the important features of deterministic chaotic systems [1–4]. Particularly, anomalous diffusion in Hamiltonian systems is of basic interest in many physical problems, for example, in mass transport and mixing in hydrodynamic flows [5–8], transport of magnetic field lines, heat and particles in fusion and space plasmas [9–11], etc. In one dimension it is characterized by a nonlinear time dependence of a mean squared displacement $\langle (\Delta x)^2 \rangle = 2Dt^{\gamma}, (\gamma \neq 1)$, while for the normal diffusion $\gamma = 1$ and D determines a diffusion coefficient.

Now it is well recognized that the anomaly of chaotic transport in deterministic Hamiltonian systems is due to the fact that a domain of chaotically unstable motion, known as a stochastic layer, is not uniform and consists of subdomains of regular motions (so called Kolmogorov-Arnold-Mozer (KAM)-stability islands). The structure of the chaotic domain, i.e., the mutual positions of KAM-stability islands and their sizes, are believed to determine the rate of anomalous transport processes. The transport analysis in such complex systems has been the subject of many investigations during the last decade (see, e.g., [4,12–14]).

In this Rapid Communication we study an anomalous chaotic transport in one-degree-of-freedom Hamiltonian system with hyperbolic fixed points subjected to time-periodic perturbations. This system is generic and has many physical applications [5–8,15–22]. Any small strength of perturbation destroys phase-space curves connecting saddle points (separatrices) and separating domains of different types of motions, and chaotic motion appears near the unperturbed separatrices. Recently the important rescaling property of perturbed motion near the hyperbolic fixed points has been established in [23–25]. It has been found that the scaling transformation (of the amplitude ϵ and the phase χ of the time-periodic perturbation) preserves the topology of the phase-space of canonical variables (x,p) near the hyperbolic fixed point. The equations of motion near the hyperbolic fixed point are invariant with respect to

$$\epsilon \to \epsilon' = \lambda \epsilon, \quad \chi \to \chi' = \chi + \pi,$$

$$x \to x' \approx \lambda^{1/2} x, \quad p \to p' \approx \lambda^{1/2} p. \tag{1}$$

The rescaling parameter λ depends only on the perturbation frequency and the property of the unperturbed Hamiltonian near the hyperbolic fixed point. This is a generic property of a one-degree-of-freedom Hamiltonian system subjected to the time-periodic perturbation, and as we shall demonstrate that it will lead to important universal consequences in chaotic transport in the system. Indeed, particles spend long time intervals near the saddle points. There they slow down, and thus transport of particles along the stochastic layer is mainly determined by the structure of the stochastic layer near the saddle point. One can expect that similar structures of the stochastic layer near these regions will be reflected in the transport properties.

To be more specific, consider as a generic model the motion of a particle trapped by a main wave subjected to disturbances by two weak waves propagating in opposite directions. This system is described by the Hamiltonian

$$H = \frac{p^2}{2} - \omega_0^2 \cos x - \epsilon \omega_0^2 [\cos(x - \nu t + \chi) + \cos(x + \nu t + \chi)], \tag{2}$$

where ω_0 is the frequency of small oscillations; ϵ and ν represent the amplitude and the frequency of the perturbation, respectively. The unperturbed system ($\epsilon = 0$) has elliptic fixed points (at $x = 2\pi n, p = 0$) and hyperbolic fixed points [at $x = 2\pi(n + 1/2), p = 0$].

Any small perturbation ($\epsilon \neq 0$) destroys the separatrix and forms a stochastic layer near the unperturbed separatrix. The structure of the stochastic layer changes with the perturbation amplitude ϵ and the phase χ. However, the phase-space topologies of the stochastic layer near the hyperbolic saddle points (x,p) are similar when two different perturbation amplitudes and phases are related through $(\epsilon, \chi) \to (\lambda \epsilon, \chi + \pi)$. The rescaling parameter λ is determined by the perturbation frequency ν and the behavior of the unperturbed Hamiltonian near the hyperbolic fixed point [23–25]. For system (2), $\lambda = \exp(2\pi\omega_0/\nu)$. This rescaling property is shown in Fig. 1 by plotting Poincaré sections for the Hamiltonian system (2) near the saddle point for: (a) $\epsilon_a = 0.02, \chi_a = 0$, and (b) $\epsilon_b = \lambda \epsilon_a = 0.08$, $\chi_b = \pi$ at the value $\lambda = 4$. The mutual positions of islands of types 1, 2, and 3 are similar,

*Present address: Institut für Plasmaphysik, Forschungszentrum Jülich GmbH, D-52425 Jülich, Germany.

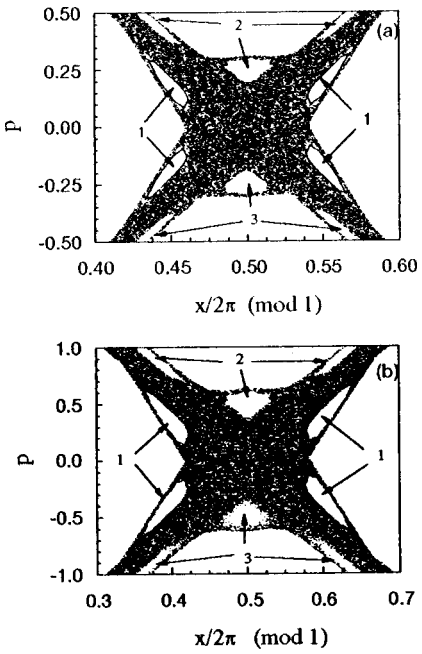

FIG. 1. Poincaré section of system (2) near the hyperbolic fixed point: (a) $\epsilon_a=0.02, \chi_a=0$, and (b) $\epsilon_b=\lambda\epsilon_a=0.08, \chi_b=\pi$. The rescaling parameter is $\lambda=4$.

the coordinates of their fixed points are related according to Eq. (1). Due to stickiness in the chaotic region near the islands of type 1 particles may be trapped for a long time while near the island 2 (or 3) particles may fly long distances along positive (or negative) direction of the x axis.

For small perturbations ϵ, the chaotic motion near the separatrix may be described by a shifted separatrix map. The latter is a return map of time (t) and energy (H) to the same section of the phase–space [24,26]. Near the separatrix, the corresponding map for the Hamiltonian system (2) has the form

$$h_{k+1}=h_k+\epsilon K\sin[\varphi_k+\nu T(h_k)/4+\chi],$$

$$\varphi_{k+1}=\varphi_k+\nu[T(h_k)+T(h_{k+1})]/4, \tag{3}$$

where $\varphi=\nu t, h=(H-\omega_0^2)/\omega_0^2$, $K=4\pi\Lambda^2/\sinh(\pi\Lambda/2)$, $\Lambda=\omega_0/\nu$, and $T(h)=2\pi/\omega(h)$ is a period of unperturbed motion, and $\omega(h)$ is its frequency. Near the separatrix, the universal asymptotics

$$T(h)=\frac{1}{\omega_0}\ln\frac{32}{|h|}+f(h), \quad \text{for } h\to\pm 0, \tag{4}$$

appears, where the correction term $f(h)$ is of order h. Such asymptotics (4) leads to a chaotic motion near the separatrix, which occurs for any small perturbation amplitude ϵ due to overlapping of infinite number of resonances of type $m\omega(h)=n\nu$, ($m=m_0,\ldots,\infty$; n is an integer number) [16]. The smallest number m_0 is determined by ϵ.

In the limit $|h|\to 0$, the separatrix map (3) is invariant with respect to the transformation (1) with the rescaling parameter $\lambda=\exp(2\pi\omega_0/\nu)$. It means that the topology of the stochastic layer is periodically repeating when changing the perturbation parameter ϵ, i.e., it is a periodic function of $\ln\epsilon$ with the period $\ln\lambda=2\pi\omega_0/\nu$. It can be expected that the

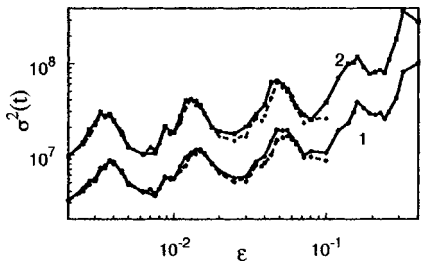

FIG. 2. Second moment $\sigma^2(t)$ vs perturbation amplitude ϵ as obtained by direct numerical integration. Solid curve 1 corresponds to $t=10^4\ T_0$ and solid curve 2 to $t=2\times10^4\ T_0(T_0=2\pi/\nu)$. The corresponding dashed curves describe the results obtained by the separatrix map (3).

periodical change of the stochastic layer topology also leads to periodical (or quasiperiodical) changes in the transport characteristics.

In order to study this effect we have considered a chaotic transport of particles along the (infinite) x axis of the stochastic layer. The second moment $\sigma^2(t)=\langle(x-\langle x\rangle)^2\rangle$ of the spatial displacement is first calculated by direct numerical integration of the Hamiltonian system (2), up to the time instant $t=2\times10^4\ T_0$ for different perturbation parameters ϵ. Here $T_0=2\pi/\nu$ is the period of the perturbation. A set of initial data ($t=0$) consisting of $N=5\times10^3$ trajectories were taken in a square region centered at the hyperbolic fixed point ($x=\pi, p=0$). Because of the fact that the perturbation in Eq. (2) acts symmetrically on particles traveling in both (positive and negative) directions along x axis, the mean value of x is expected to be $\langle x\rangle=0$.

Since the numerical integration of the Hamiltonian system is rather time consuming, we have also used as a second approach the separatrix map (3) to calculate $\sigma^2(t)$. The latter is almost three orders of magnitude faster. It is also applied to obtain the probability density function (PDF) $P(x,t)$ for a particle with position x at time instant t.

The dependence of $\sigma^2(t)=\langle(x-\langle x\rangle)^2\rangle$ on the perturbation amplitude ϵ is shown in Fig. 2 at two different time instants: solid curve 1 corresponds to $t=10^4\ T_0$ and solid curve 2 to $t=2\times10^4\ T_0$. The perturbation frequency is chosen as $\nu=4.53236\omega_0$. Then the rescaling parameter is $\lambda=4$. The variance $\sigma^2(t)$ was also calculated using the separatrix map (3) [with an average over $N=10^4$ orbits]. The dashed curves in Fig. 2 correspond to the latter calculations. The map (3) correctly reproduces the results of direct numerical integrations, with a good accuracy up to the value $\epsilon=0.1$.

Figure 2 clearly shows the strong quasi-periodical dependence of the second moment $\sigma^2(t)$ on the perturbation parameter ϵ. There are local maxima of $\sigma^2(t)$ at the values $\epsilon_{max}^{(j)}=\lambda^{-j}\epsilon_{max}$, $\epsilon_{max}\approx0.192$, and local minima at $\epsilon_{min}^{(j)}=\lambda^{-j}\epsilon_{min}, \epsilon_{min}\approx0.08$, ($j=1,2,\ldots$). For large perturbation amplitudes $\epsilon>0.1$ the quasi-periodical behavior of $\sigma^2(t)$ is less pronounced since the rescaling property of Hamiltonian system starts to violate for large perturbations.

The behavior of the second moment $\sigma^2(t)$ for long times $t>2\times10^4$ was studied using the separatrix map (3). Figure 3 shows $\sigma^2(t)$ versus ϵ at the different time instants $t/T_0=10^4, 2\times10^4, 5\times10^4, 10^5, 10^6$, continuously numbered 1 to 5, respectively. With increasing time, the periodic depen-

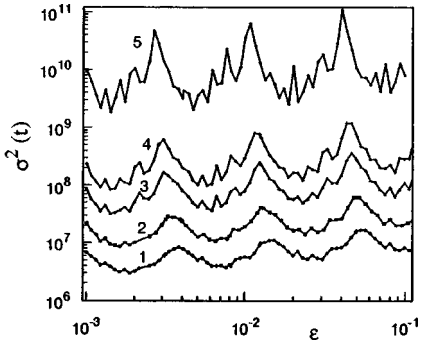

FIG. 3. Same as in Fig. 2, but for the time instants: $t=10^4\ T_0$ (1), $2\times10^4\ T_0$ (2), $5\times10^4\ T_0$ (3), $10^5\ T_0$ (4), $10^6\ T_0$ (5).

dence of $\sigma^2(t)$ on ϵ becomes more pronounced.

The profiles near the maxima become sharper, with shallow regions between them. The positions of the maxima $\epsilon_{max}^{(j)}$ move towards smaller ϵ, but the positions of the minima $\epsilon_{min}^{(j)}$ become less distinct. The sharp maxima are due to the crossing the critical perturbation amplitude $\epsilon_{mn}^{(-)}$ for destruction of the last KAM-invariant curve between the stochastic layer and the $m:n$ resonance of type 1 (islands of type 1 in Fig. 1), i.e., $m\omega(h_{mn})=n\nu,(h_{mn}<0)$, with the smallest possible number m. Just before crossing the invariant curve, more orbits are trapped by islands of type 2 and 3. The reason is that the corresponding critical perturbation amplitude $\epsilon_{mn}^{(+)}$ for these resonances $[m\omega(h_{mn})=n\nu,h_{mn}>0]$, is smaller than for the resonance of type 1, i.e., $\epsilon_{mn}^{(+)}<\epsilon_{mn}^{(-)}$. This asymmetry is due to the correction term $f(h)$ in Eq. (4). It results in enhancing the transport rate along the x axis. After crossing the critical $\epsilon_{mn}^{(-)}$, the resonance $m:n(h_{mn}<0)$ joins to the stochastic layer, and orbits start to be trapped by that resonance. This leads to the decreasing of the transport rate. The small amplitude oscillations in $\sigma^2(t)$ with respect to ϵ are due to the joining of $m:n$ resonances with higher numbers m. The long time evolution more precisely reveals the existence of critical perturbation amplitudes $\epsilon_{mn}^{(\pm)}$ for destruction of KAM-invariant curves between the stochastic layer and the $m:n$ resonance.

For large times t the asymptotics is $\sigma^2(t)\sim t^\gamma$. The exponent γ is also a strong quasiperiodic function of $\ln\epsilon$ with the period $\ln\lambda$. The dependence γ on ϵ obtained using the separatrix map (3) is shown in Fig. 4. The chaotic transport along the x axis is superdiffusive ($\gamma>1$) for all perturbation amplitudes. The exponent γ takes maximum and minimum values at the same ϵ values as $\sigma^2(t)$ does. The regions with $\gamma>2$ correspond to the acceleration regimes.

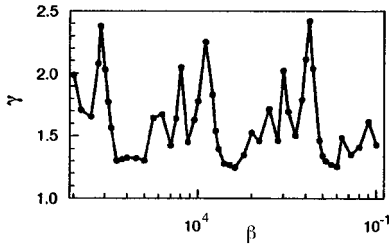

FIG. 4. Exponent γ vs perturbation amplitude ϵ. It is obtained by fitting $\sigma^2(t)$ with $2Dt^\gamma$ in the large time interval $10^4\ T_0\leqslant t\leqslant10^5\ T_0$.

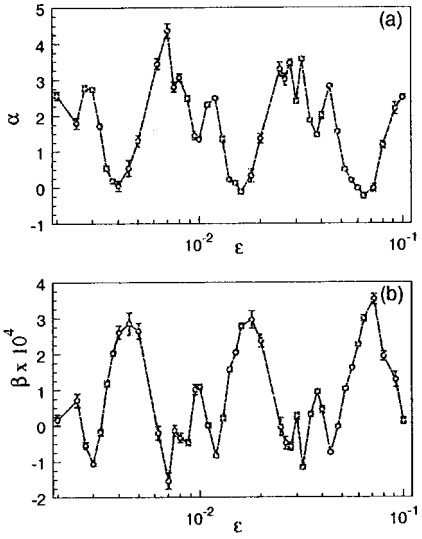

FIG. 5. Fitting parameters α and β for a power-exponential law $P(x,t)\sim|x|^{-\alpha}\exp(-\beta|x|)$: (a) α vs ϵ; (b) β vs ϵ. A time instant $t=2\times10^4\ T_0$.

The separatrix map (3) is also applied to calculate PDF $P(x,t)$. The PDF $P(x,t)$ was calculated at the time instant $t=2\times10^4\ T_0$ for perturbation parameters ϵ in the interval $[0.002, 0.1]$. The number of orbits is $N=10^5$. The PDF is almost symmetric with respect to $x=0$, and it is mostly localized near this point. The width $2\Delta\sigma$ of $P(x,t)$ defined as an area $-\Delta\sigma<x<\Delta\sigma$, where a half of orbits is localized, i.e., $\int_{-\Delta\sigma}^{\Delta\sigma}P(x,t)dx=0.5$, has also a strong periodical dependence on $\ln\epsilon$ similar to $\sigma^2(t)$.

The main feature of $P(x,t)$ is its long tail asymptotics for $|x|\gg\Delta\sigma$. The latter significantly depends on the perturbation parameter ϵ. The comparison, for instance, of the two PDF at $\epsilon=0.048$ and $\epsilon=0.08$ for which the second moments $\sigma(t)$ have maximum and minimum values, respectively, shows that while the PDF for $\epsilon=0.048$ has a slowly decaying tail, the PDF for $\epsilon=0.08$ decays much faster. We have approximated $P(x,t)$ asymptotically by power exponential, $P(x,t)\sim|x|^{-\alpha}e^{-\beta|x|}$,law. The fitting exponents α and β at the time instant $t=2\times10^4\ T_0$ are presented in Fig. 5: (a) shows α versus ϵ, while (b) shows β versus ϵ. First of all, a strong quasiperiodic dependence of these parameters on $\log\epsilon$ appears with the period $\log\lambda$ similar to that for the exponent γ in the time–asymptotics of $\sigma^2(t)$.

There are regions of ϵ at the minima of $\sigma^2(t)$ where the parameter $|\beta|$ is relatively small, and the tail of PDF is more closely described by the powerlike law $|x|^{-\alpha}$. At the growing phases of the quasiperiodical dependence of $\sigma^2(t)$ on ϵ the parameter β may take even negative values, which means that tail of PDF decays even slower than the powerlike law $|x|^{-\alpha}$ (see Fig. 2). On the other hand, the exponential decrease $e^{-\beta|x|}$ of $P(x,t)$ prevails in the regions of ϵ where $\sigma^2(t)$ is decreasing. The exponential decrease of the probability to find particles at large x is due to trapping of particles by the $m:n$ resonance with the smallest possible number m (the island of type 1 in Fig. 1) (when ϵ crosses the critical value $\epsilon_{mn}^{(-)}$ for destruction of the last KAM-invariant curve between the stochastic layer and the $m:n$ resonance). On the other hand, for $\epsilon<\epsilon_{mn}^{(-)}$, particles are trapped by

resonances of type 2 and 3, and therefore they can travel long distances x. In this case, the tail of $P(x,t)$ decays slower than $|x|^{-\alpha}$. Overall the results show that the asymptotics of PDF $P(x,t)$ for $|x| \gg \Delta\sigma$ significantly depends the structure of the stochastic layer, and it is mainly determined by the outermost KAM-stability islands at the chaos border.

In conclusion, we have established a strong quasiperiodical dependence of transport properties on the perturbation parameter. This effect is universal for one-degree-of-freedom Hamiltonian system subjected to small time-periodic perturbation regardless on the specific features of the system. One can expect the effect occurs, for instance, in chaotic mass transport in a chain of vortices in a shear layer [8], planar periodic vortical flows [21]. Similar it may be also observed in models of physical systems which are described by a stochastic web (see, e.g., [4]).

It also suggests that the chaotic transport does not monotonically increase with the perturbation amplitude, as it is often assumed in qualitative transport. The established effect shows the possible range of controlling Hamiltonian chaos [27], in particularly, the chaotic transport by varying the perturbation amplitude. It may be useful to control a transport of heat and particles in magnetic fusion devices with stochastic magnetic field lines [28], a transport of passive scalars in a chain of vortices [8], or a mixing of fluids [22].

S.A gratefully acknowledges generous support and valuable comments of Professor G. Eilenberger.

[1] C.F.F. Karney, Physica D **8**, 360 (1983).
[2] B.V. Chirikov and D.L. Shepelyansky, Physica D **13**, 395 (1984); B.V. Chirikov, Chaos, Solitons and Fractals **1**, 79 (1991).
[3] J.-P. Bouchaud and A. Georges, Phys. Rep. **195**, 127 (1990).
[4] M.F. Shlesinger, G.M. Zaslavsky, and J. Klafter, Nature (London) **363**, 31 (1993); J. Klafter, M.F. Shlesinger, and G. Zumofen, Phys. Today **49**(2), 33 (1996).
[5] J.B. Weiss, and E. Knobloch, Phys. Rev. A **40**, 2579 (1989).
[6] J.B. Weiss, Phys. Fluids A **3**, 1379 (1991).
[7] E. Weeks, J.S. Urbach, and H. Swinney, Physica D **97**, 291 (1996).
[8] D. del Castillo-Negrete, Phys. Fluids **10**, 576 (1998).
[9] R. Balescu, Phys. Rev. E **51**, 4807 (1995).
[10] G. Zimbardo and P. Veltri, Phys. Rev. E **51**, 1412 (1995).
[11] F.D. Angelo and R. Paccagnella, Phys. Plasmas **3**, 2353 (1996).
[12] G.M. Zaslavsky, D. Stevens, and H. Weitzner, Phys. Rev. E **48**, 1683 (1993).
[13] G. Zumofen and J. Klafter, Phys. Rev. E **47**, 851 (1993); J. Klafter and G. Zumofen, *ibid.* **49**, 4873 (1994).
[14] R. Balescu, Phys. Rev. E **55**, 2465 (1997).
[15] N.N. Filonenko and G.M. Zaslavsky, Sov. Phys. JETP **25**, 851 (1968).
[16] B.V. Chirikov, Phys. Rep. **52**, 256 (1979).
[17] *Hamiltonian Dynamical Systems - A Reprint Selection*, edited by R.S. MacKay and J.D. Meiss (Adam Hilger, Bristol, 1987).
[18] D.F. Escande, Phys. Rep. **121**, 165 (1985).
[19] D.F. Escande, in *Proceedings of the International Workshop, Kiev, 1987*, edited by V.G. Bar'yakhtar, V.M. Chernousenko, N.S. Erokhin, A.G. Sitenko, and A.V. Zakharov (World Scientific, Singapore, 1988), pp. 398–430.
[20] A. Lichtenberg and B. Wood, Phys. Rev. A **39**, 2153 (1989).
[21] T. Ahn and S. Kim, Phys. Rev. E **49**, 2900 (1994).
[22] J.M. Ottino, *The Kinematics of Mixing: Stretching, Chaos, and Transport*, (Cambridge University Press, Cambridge, England, 1989).
[23] S.S. Abdullaev and G.M. Zaslavsky, Bull. Am. Phys. Soc. **39**, 1659 (1994); G.M. Zaslavsky and S.S. Abdullaev, Phys. Rev. E **51**, 3901 (1995).
[24] S.S. Abdullaev and G.M. Zaslavsky, Phys. Plasmas **2**, 4533 (1995).
[25] S.S. Abdullaev, Phys. Lett. A **234**, 281 (1997).
[26] S.S. Abdullaev and G.M. Zaslavsky, Phys. Plasmas **3**, 516 (1996).
[27] Y.-C. Lai, M. Ding, and C. Grebogi, Phys. Rev. E **47**, 86 (1993).
[28] Ph. Ghendrih, A. Grosman, and H. Capes, Plasma Phys. Controlled Fusion **38**, 1653 (1996).